Ultrasmall multi-port channel drop filter in two-dimensional photonic crystal on silicon-on-insulator substrate

Akihiko Shinya, Satoshi Mitsugi, Eiichi Kuramochi, and Masaya Notomi

NTT Basic Research Laboratories, Nippon Telegraph and Telephone Corporation, 3-1, Morinosato Wakamiya, Atsugi, 243-0198, Japan
shinya@nttbrl.jp

Abstract: We demonstrate ultrasmall five-port channel drop filters (CDFs) based on a two-dimensional photonic crystal slab. We combine seven photonic crystals with different lattice constants and use light reflections at the different photonic crystal boundaries to control the interference process and achieve a high dropping efficiency. We operate the CDFs in two modes; one requires careful control of the interference process, whereas the other does not. The former can output a narrower signal spectrum than the latter, and CDF design is easier with the latter. Both CDFs achieve a high dropping efficiency and can function in the CL-band.

OCIS codes: (250.5300) Photonic integrated circuits; (230.7370) Waveguides; (230.5750) Resonators; (230.3990) Microstructure devices.

References and links

1. B. S. Song, S. Noda, and T. Asano, "Photonic devices based on In-plane hetero photonic crystals," Science **300**, 1537 (2003).
2. A. Shinya, S. Mitsugi, E. Kuramochi, M. Notomi, "Ultrasmall multi-channel resonant-tunneling filter using mode gap of width-tuned photonic-crystal waveguide," Opt. Express **13**, 4202-4209 (2005). http://www.opticsinfobase.org/abstract.cfm?URI=oe-13-11-4202
3. H. Takano, B-S. Song, T. Asano, S. Noda, "Highly efficient multi-channel drop filter in a two-dimensional hetero photonic crystal," Opt. Express, **14**, 3491-3496 (2006). http://www.opticsinfobase.org/abstract.cfm?URI=oe-14-8-3491
4. H. Takano, B. S. Song, T. Asano, and S. Noda, "Highly efficient in-plane channel drop filter in a two-dimensional heterophotonic crystal," Appl. Phys. Lett. **86**, 241101 (2005)
5. S. Fan, P. R. Villeneuve, J. D. Joannopoulos, "Channel drop tunneling through localized states," Phys. Rev. Lett. **80**, 960-963 (1998).
6. H. Takano, Y. Akahane, T. Asano, and S. Noda, "In-plane-type channel drop filter in a two-dimensional photonic crystal slab," Appl. Phys. Lett. **84**, 2226-2228 (2004).
7. A. Shinya, S. Mitsugi, T. Tanabe, M. Notomi, I. Yokohama, H. Takara, S. Kawanishi, "All-optical flip-flop circuit composed of coupled two-port resonant tunneling filter in two-dimensional photonic crystal slab," Opt. Express **14**, 1230-1235 (2006). http://www.opticsinfobase.org/abstract.cfm?URI=oe-14-3-1230
8. M. Notomi, A. Shinya, S. Mitsugi, G. Kira, E. Kuramochi, and T. Tanabe, "Optical bistable switching action of Si high-Q photonic-crystal nanocavities," Opt. Express **13**, 2678-2687 (2005). http://www.opticsexpress.org/abstract.cfm?URI=OPEX-13-7-2678
9. M. F. Yanik, S. Fan, and M. Soljacic, "High-contrast all-optical bistable switching in photonic crystal microcavities," Appl. Phys. Lett. **83**, 2739-2741 (2003).
10. T. Tanabe, M. Notomi, S. Mitsugi, A. Shinya, and E. Kuramochi, "All-optical switches on silicon chip realized using photonic crystal nanocavities," Appl. Phys Lett. **87**, 15112 (2005).
11. T. Tanabe, M. Notomi, S. Mitsugi, A. Shinya, and E. Kuramochi, "Fast bistable all-optical switch and memory on silicon photonic crystal on-chip, " Opt. Lett. **30,** 2575 (2005).
12. E. Kuramochi, M. Notomi, S. Mitsugi, A. Shinya, T. Tanabe, and T. Watanabe, "Ultrahigh-Q photonic crystal nanocavities realized by the local width modulation of a line defect," Appl. Phys. Lett. **88**, 041112 (2006).
13. M. Notomi, A. Shinya, S. Mitsugi, E. Kuramochi, and H-Y. Ryu, "Waveguides, resonators and their coupled elements in photonic crystal slabs," Opt. Express **12**, 1551-1561 (2004). http://www.opticsexpress.org/abstract.cfm?URI=OPEX-12-8-1551

#74743 - $15.00 USD Received 5 September 2006; revised 29 September 2006; accepted 19 October 2006

14. G-H Kim, Y-H Lee, A. Shinya, and M. Notomi, "Coupling of small, low-loss hexapole mode with photonic crystal slab waveguide mode," Opt. Express **26**, 6624-6631 (2004). http://www.opticsexpress.org/abstract.cfm?URI=OPEX-12-26-6624

1. Introduction

Photonic crystals (PhC) are expected to provide a platform for future photonic integrated circuits. The advantage of using a PhC is that we can realize an ultrasmall resonator with a high quality factor (Q-factor), which can be effectively connected to single-mode waveguides in the PhC. Such a coupled resonator-waveguide system can function as a resonant tunneling filter, and is widely used in newly proposed optical devices [1-14].

One of the most important PhC devices is the channel drop filter (CDF) [1-6]. The simplest way to construct a CDF is to install a resonator between two waveguides. The input light from one waveguide is resonated with the resonator, and then output from the other waveguide. In this case, the dropping efficiency is only 25% because the light is output from the four ends (ports) of the two waveguides and so is unsuitable for a CDF. Several structures have been reported with a view to solving this problem [1-5]. But the fabricated devices are not very small [1, 3-4], and so they do not exploit the advantage of PhCs with respect to minimizing device size. The problem is the arrangement of the waveguides and resonators. For example, Takano et al [3, 4] describe an excellent way of achieving output signal uniformity in PhC based CDFs by connecting some PhCs with different lattice constants. But they use bent waveguides as drop waveguides, which makes the device size large. And since they use an interference process to improve the dropping efficiency, it is necessary to handle the phase relation carefully. On the other hand, we have proposed a way of narrowing the interval of drop waveguides and an idea for improving the dropping efficiency without the need for careful handling of the phase relation [2]. However, it is not easy to achieve output signal uniformity in a real device because only one PhC is used. In this report, we combine the advantages described in [2] and [3] and demonstrate ultrasmall CDFs with a size of about 18 μm. These CDFs are composed of seven different PhCs to make use of the reflection between different PhCs, and can separate five signals with different wavelengths.

2. Design and discussion

Figure 1 is a scanning electron micrograph of our sample. It is fabricated on a silicon-on-insulator substrate by a combination of electron beam lithography and inductively coupled plasma dry etching. It is composed of seven different PhCs with different lattice constants. The solid lines show the boundaries between them. The seven PhCs are arranged from left to right with their lattice constants in descending order. And a bus waveguide passes through the connected PhCs, and five resonators and five dropping waveguides are arranged beside the bus waveguide. The lattice constant of the second PhC is 420 nm and the distance between the first and the fifth resonator is only about 18 μm.

The structures of the resonators and the waveguides are shown in Fig. 2. The resonant frequency of the resonator and the propagation band frequency of the waveguide are optimized by tuning their widths W_c and W. The structures of the resonators and waveguides are similar in each PhC, and their resonant frequencies and band frequencies are inversely proportional to their size. Here, the lattice constants decrease in decrements of 2% from left to right, which means that five signals are dropped by five resonators with a wavelength separation of about 30 nm in the CL-band.

#74743 - $15.00 USD Received 5 September 2006; revised 29 September 2006; accepted 19 October 2006

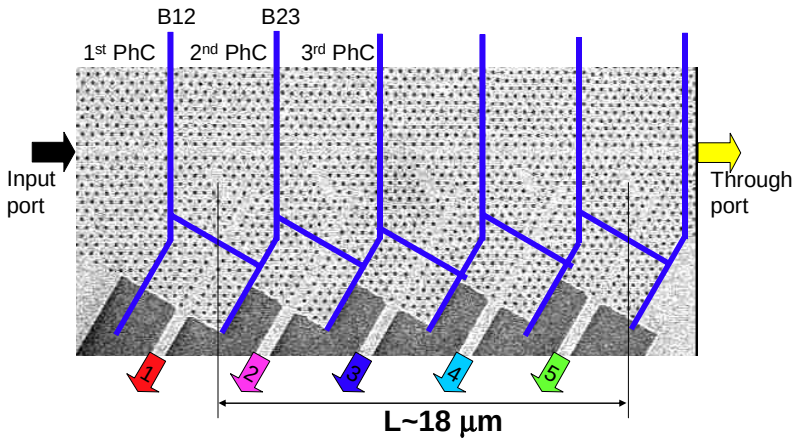

Fig. 1. Scanning electron micrograph of our sample. The slab is about 200 nm thick and the air hole diameter is about 210 nm. The solid lines show the boundaries between the seven different PhCs. Seven PhCs are arranged from left to right in descending order of lattice constant. The lattice constant of the second PhC is 420 nm. The lattice constants decrease in decrements of 2% from left to right. The device size from the first to the fifth resonator is only about 18 μm.

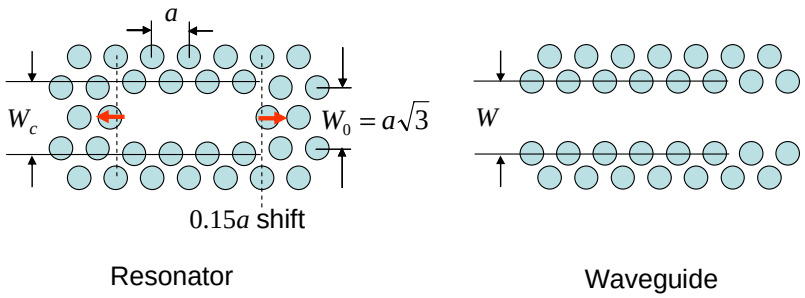

Fig. 2. Structures of the waveguides and the resonators. W_c and W are the widths of the resonator and the waveguide. a is the lattice constant of the PhC. The position of the innermost hole in the resonator is optimized to increase the Q-factor [6].

The operating mechanism of our CDF can be explained by using structures combining two different PhCs (PhC_A and PhC_B) with different lattice constants as shown in Fig. 3. Figure 3(a) and (b) show the schematic structures of CDFs operating in two different operating modes (mode 1 [3-4] and mode 2 [2]). For ease of understanding, the equivalent structures of Fig. 3(a) and (b) are shown in Fig. 3(c) and (d), respectively.

Mode 1 operation can be achieved in a coupled resonator-waveguide system in which one resonator is installed between two waveguides in PhC_A, and PhC_B is connected to PhC_A as shown in Fig 3(c). The structure is tuned so that the light resonating with the resonator cannot propagate in the waveguide in PhC_B, and the light reflected at the boundary between two PhCs after passing through the side of the resonator, destructively interferes with the light output from the resonator to the input port after being trapped in the resonator. As a result, the output to the input port is eliminated and the light is output from only one port [2, 3].

Mode 2 operation can be achieved in a similar system to that used for mode 1. The difference is that the resonator is arranged in PhC_B as shown in Fig. 3(d). Here, the phase difference between the light reflected at the boundary between two PhCs and the light output from the resonator to the input port is π. As a result, the output to the input is always canceled and the light is output from only one port. In short, it is not necessary to optimize the phase

#74743 - $15.00 USD Received 5 September 2006; revised 29 September 2006; accepted 19 October 2006

relation to make the interference destructive, which means that it is easier to design a CDF operating in mode 2 than in mode 1 [2].

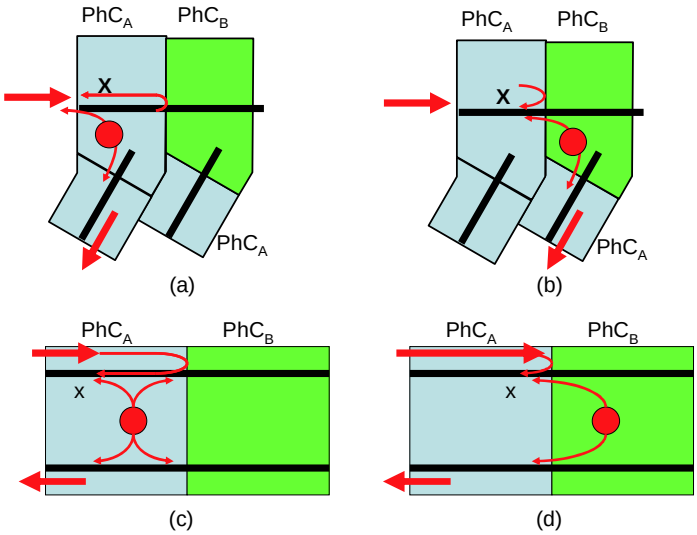

Fig. 3. (a) and (b) show the schematic structures of CDFs operating in modes 1 and 2. The lattice constant of PhC_A is larger than that of PhC_B. (c) and (d) are the equivalent structures of (a) and (b), respectively. The light resonating with the resonator cannot propagate through the waveguide in PhC_B.

Figure 4 shows the transmission spectra of a CDF operating in mode 1. Here, $W = 1.00W_0$, and $W_c = 1.00W_0$, where $W_0 = a\sqrt{3}$, and a is the lattice constant of the PhC. The black line is the transmission spectrum of the waveguide in the first PhC (WG1) in Fig. 1. The band edge of the long wavelength side of WG1 is about 1610 nm. A signal whose wavelength is longer than the edge cannot propagate in WG1. The band edge of the waveguide in the second PhC (WG2) is at a longer wavelength than the resonant wavelength of the resonator in the second PhC (C2). Moreover, the band edge of the waveguide in the third PhC (WG3) is set between the resonant wavelengths of C2 and the resonator in the third PhC (C3). The wavelengths of these band edges are proportional to their lattice constants. As a result, light resonating with C2 can propagate in WG1 and WG2, but not in WG3. Therefore, the light is reflected back at the boundary between WG2 and WG3 (B23) with the trapped light output from C2. Since we set the distance between B23 and C2 so that the interference was destructive, we achieved a high dropping efficiency at each drop port. A CDF operating in mode 1 has already been reported in [3], however our CDF is much smaller. The difference between them is the PhC arrangement. The CDF in [3] uses the structure shown in Fig. 3(c). In contrast, we use the structure shown in Fig. 3(a) with slanted waveguides, which makes the device length from the first to the last resonator shorter than that in [3].

It is not easy to calculate the transmittance, because transmission spectra are affected by Fabry-Perot interference due to the reflections at a facet plane of the device, and at the ends of the bus and the drop waveguides. Here, we normalized the output signal by the envelope of the WG1 spectrum to estimate the transmittance. The envelope is a line connecting the peaks of the Fabry-Perot interference ripples. The dropping efficiency is the maximum value of the normalized signal and the line width is the FWHM of the spectrum. Here, we cannot calculate the dropping efficiency when the wavelength is shorter than the dip in the WG1 spectrum around 1475 nm. In this wavelength region, the propagation loss of the WG1 becomes large due to the air light cone. Since the length of WG1 for reference is about 35 μm, which is much longer than the length of WG1 in CDF, we cannot use the WG1 spectrum to normalize

#74743 - $15.00 USD Received 5 September 2006; revised 29 September 2006; accepted 19 October 2006

the signals. We estimated the average dropping efficiency and average line width to be 74.6% and 4.1 nm, respectively. The dropping efficiency is much larger than the value of 25% for a simply coupled system.

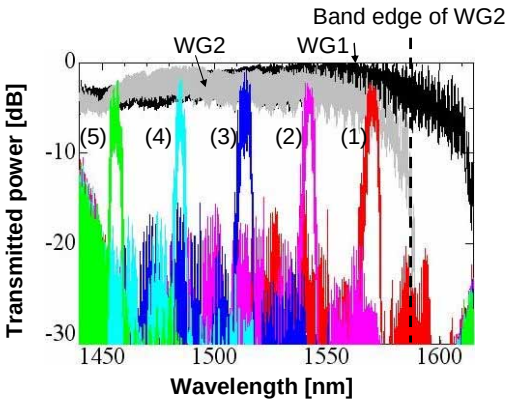

Fig. 4. Transmission spectra of CDF operating in mode 1. $W = 1.00W_0$, $W_c = 1.00W_0$. The black and gray lines are the transmission spectra of the waveguides in the first PhC (WG1) and the second PhC (WG2). (1) The red, (2) magenta, (3) blue, (4) cyan, and (5) green signals are output from the left to the right drop waveguides in Fig. 1. The dotted line is the band edge of the long wavelength side of WG2. The red signal is on the left hand side of the band edge of WG2. The center wavelengths of the signals are 1569,1540,1513,1485,1457 nm, their line widths are 4.4, 4.2, 4.8, 2.6, 4.3 nm, and their transmittances are 61.5, 60.0 89.1, 87.6 %. The transmittance of port 5 is not calculated.

Figure 5 shows the transmission spectra of a CDF operating in mode 2. Here, $W = 0.98W_0$, and $W_c = 1.05W_0$. In this case, the resonant wavelength of C2 is set between the band edges of WG1 and WG2 by tuning the width of the waveguides so that they are narrower than those for mode 1. As a result, the light resonating with C2 can propagate only in WG1, therefore, a part of the input light is reflected back at the boundary between WG1 and WG2 (B12). Moreover, another part of the input light is trapped in C2 and reflected back to WG1. Since the phase difference between these two lights in WG1 is always π, the reflection toward the input port is always eliminated, and a high dropping efficiency is achieved at each drop port. As far as we know, this is the first experimental result report of a multi-port CDF operating in mode 2. We estimated the average dropping efficiency and average line width to be 89.8% and 7.8 nm, respectively. The dropping efficiency is higher than that in Fig. 4.

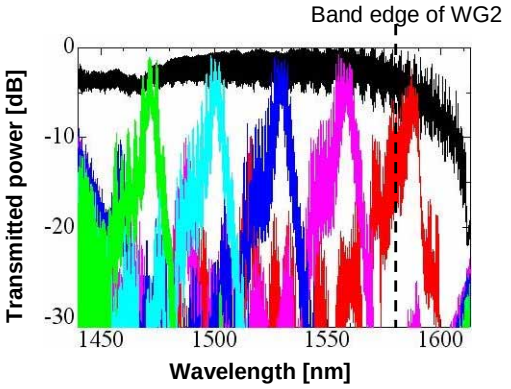

Fig. 5. Transmission spectra of a CDF operating in mode 2. $W = 0.98W_0$, $W_c = 1.05W_0$. The red signal is on the right hand side of the band edge of WG2. The center wavelengths of the signals are 1587, 1555, 1528, 1499, 1471 nm, their line widths are 6.2, 8.3 7.9, 8.3, 8.2 nm, and their transmittances are 99.8, 77.9, 86.3, 95.3 %. The transmittance of port 5 is not calculated.

#74743 - $15.00 USD Received 5 September 2006; revised 29 September 2006; accepted 19 October 2006

It should be noted that the width of the transmission spectra in Fig. 4 is narrower than that in Fig. 5. In the resonant tunneling filter, the line width is inversely proportional to the Q factor of the filter, which is determined by Q_v and Q_H [13, 14]. Here, Q_v is the intrinsic Q factor of the resonator. Q_H is determined by the coupling coefficient between the waveguides, and the resonator and is inversely proportional to the distance between the resonator and the waveguides. As shown in Fig. 3(a) and (b), the resonating mode couples with the waveguide mode in PhC_A. Since the distance between the resonator and the waveguide in PhC_A of mode 2 is wider than that of mode 1 and the Q_H of mode 2 is larger than that of mode 1, the line width of mode 2 should be narrower than that of mode 1. However, this is not the case because of the interference between the light reflected back at the waveguide boundary and the light output from the resonator [3]. For further discussion, we show the transmission spectra of a CDF whose interference condition is different from that in Fig. 4. We change the condition by changing W from $1.00W_0$ to $0.98W_0$ in Fig. 6. The dropping efficiency is decreased at the wavelength indicated by arrows in Fig. 6, and the line width becomes narrow and its shape becomes non-symmetric. This is due to constructive interference. Destructive interference eliminates the reflection to the input port and the dropping efficiency is maximized in Fig. 4. But, when the phase relation is misaligned, constructive interference occurs and the dropping efficiency is decreased as shown in Fig. 2(a) in Ref. 4. In Fig. 6, both types of interference occur in one dropped signal and deep dips appear in the spectrum as shown in Fig. 3(a) in [2]. Such a situation easily arises when the line width is wide. This is why the line width in Fig. 4 is narrower than that in Fig. 5. Probably, constructive interference occurs at two different wavelengths in our CDFs because the filter structure is non-symmetric as described in [2] and the interference conditions in the bus waveguide and the drop waveguide are different, which may make the dropping efficiency of mode 1 lower than that of mode 2. In short, the phase relation must be carefully handled when the CDF is operating in mode 1. On the other hand, this suggests that careful design will enable us to use a narrowed spectrum, which can suppress the crosstalk between the output signals. We estimate the average dropping efficiency and average line width to be 61.5% and 2.6 nm, respectively.

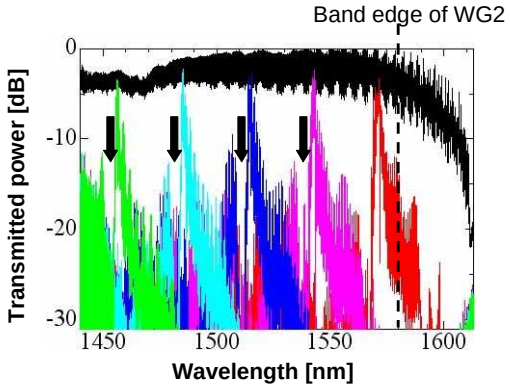

Fig. 6. Transmission spectra of CDF operating in mode 1 with a misaligned interference condition. $W = 0.98W_0$, $W_c = 1.00W_0$. The dropping efficiency is reduced at the wavelengths indicated by the arrows. The center wavelengths of signals are 1572, 1543, 1515, 1485, 1456 nm, their line widths are 3.6, 2.7, 2.9, 1.5, 2.1 nm, and their transmittances are 52.7, 58.8 58.9, 75.5 %. The transmittance of port 5 is not calculated.

It is necessary to reduce the separation wavelength of the dropped signal to increase the number of drop signals per unit wavelength. Since the separation is proportional to the variation in the lattice constant, we changed it from 2% to 1%. In this case, since the modification of the lattice constant reduces the strains between different PhCs with different lattice constants, the scattering loss caused by the strains may be suppressed. The transmission spectra of CDFs operating in modes 1 and 2 are shown in Fig. 7(a) and (b), respectively. Both

#74743 - $15.00 USD Received 5 September 2006; revised 29 September 2006; accepted 19 October 2006

figures show that the CDF can function with a high dropping efficiency of almost the same value as that found in Figs. 4 and 5. This is because the loss induced by the strains is very small [3] and the resonator loss is dominant. We estimated the average dropping efficiency and average line width to be 65.2% and 3.8 nm, respectively, for mode 1, and 78.5% and 11.4 nm, respectively, for mode 2.

For further signal multiplexing, we must decrease the separation between the edge wavelength of a waveguide and resonant wavelength of the resonator. This is easily controlled by W and W_c. Moreover, a narrower transmission spectrum line width and small area device integration are needed to realize more channels with a smaller device size. The narrow line width is easily realized by increasing the separation between the resonator and waveguide of PhC_A in Fig. 3 to increase the Q_H. In terms of integration, a CDF operating in mode 2 is more advantageous than one operating in mode 1 because we can easily design the structure of the CDF operating in mode 2 to increase the separation between the resonator and PhC_A waveguide while keeping a short distance between the bus waveguide and the dropping waveguide.

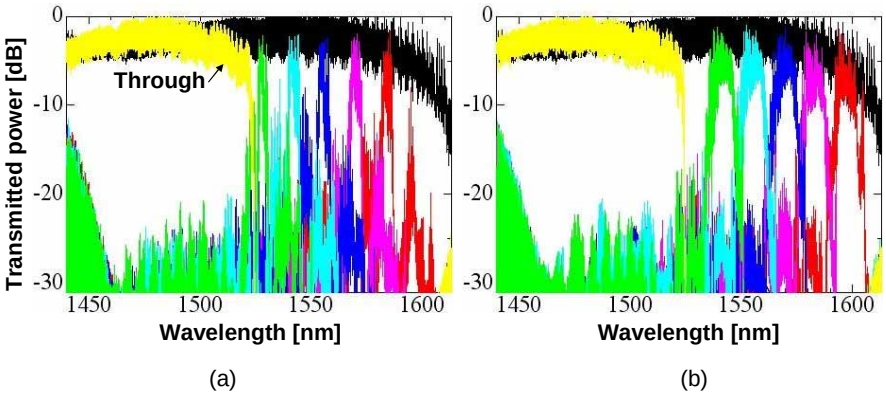

Fig. 7. Transmission spectra of CDFs operating in modes 1 and 2. The variation in the lattice constant is set at 1%. The yellow lines are the transmission spectra at the through port. (a) CDF operating in mode 1. $W = 1.00W_0$, $W_c = 1.00W_0$. The center wavelengths of signals are 1586, 1571, 1558, 1544, 1528, 1472 nm, their line widths are 2.6, 4.3, 4.6, 4.4, 3.3 nm, and their transmittances are 82.3, 68.0, 54.8, 61.3, 59.4 %. (b) CDF operating in mode 2. $W = 1.00W_0$, $W_c = 1.05W_0$. The center wavelengths of signals are 1594, 1584, 1570, 1552, 1539, 1472 nm, their line widths are 10.1, 11.4, 11.5, 11.5, 12.6 nm, and their transmittances are 100, 72.5, 71.7, 71.3, 77.0 %.

3. Conclusion

We demonstrated ultrasmall CDFs based on 2D-PhCs fabricated on SOI substrates. They have five drop ports and one through port within an 18 μm device size. And we successfully operated them in two operation modes. One is advantageous in terms of suppressing the crosstalk between dropped signals. With the other, CDF design is easier because it does not require careful handling of the interference processes to achieve a high dropping efficiency. Both CDFs achieve a high dropping efficiency and can function in the CL-band. These results show the ability of 2D-PhCs to integrate ultrasmall photonic circuits.

#74743 - $15.00 USD Received 5 September 2006; revised 29 September 2006; accepted 19 October 2006